Title

The Association of Amyloid Plaque Count with a Decrease in the Complexity of the BOLD Signal Observed in Alzheimer's Disease

Permalink

https://escholarship.org/uc/item/8hk080bn

Author

Conner, Lindsay Brittony

Publication Date

2013

Peer reviewed|Thesis/dissertation

The Association of Amyloid Plaque Count with a Decrease in the
Complexity of the BOLD Signal Observed in Alzheimer's Disease

by

Lindsay Conner

THESIS

Submitted in partial satisfaction of the requirements for the degree of

MASTER OF SCIENCE

in

Biomedical Imaging

in the

GRADUATE DIVISION

of the

UNIVERSITY OF CALIFORNIA, SAN FRANCISCO

Acknowledgement

I would like to thank my Supervisor, Dr. Norbert Schuff, as well as the members of my thesis committee, Dr. David Saloner, Dr. Duygu Tosun, and Dr. Xiaojuan Li, for their invaluable assistance in this process. I would also like to acknowledge the help of the members of the Center for Imaging of Neurodegenerative Diseases (CIND), namely Dr. Yinan Liu, who developed the method that served as the foundation for this study.

***The Association of Amyloid Plaque Count with a Decrease in the Complexity
of the BOLD Signal Observed in Alzheimer's Disease
Lindsay Conner***

Abstract

Alzheimer's disease (AD) is a prevalent degenerative disease that is both idiopathic and highly debilitating, calling for early detection and intervention before extensive irreversible brain damage occurs. Here, a novel functional complexity measure based on information theory was applied to mark a disease-related reduction in stochastic low frequency (0.01-0.08 Hz) BOLD signal fluctuations at rest. As AD progresses, BOLD signal complexity is expected to decrease in affected regions, alongside an overall increase in brain amyloid burden.

In this study, a retrospective analysis was performed on ^{18}F-AV-45 PET and rs-fMRI data from 65 subjects (30 males, 35 females; mean age ± SD: 74 ± 7.4 years), across four clinical groups (Control, Early Mild Cognitive Impairment (EMCI), MCI, and AD). The regional BOLD signal complexity measures, or transient information (TI) values, were determined from the change in uncertainty of BOLD pattern prediction over time (i.e. block entropy growth rate).

The main findings in this study included an expected regional reduction in functional complexity with increasing amyloid burden, as well as an unexpected, albeit non-significant, global increase in functional complexity with increased amyloid burden and disease progression. One third (27 out of 82) of the cortical and subcortical grey matter regions presented a significant (>90% CI) effect of brain amyloid load on BOLD signal complexity, including regions associated with disease-

related dysfunction in memory, language processing, attention, behavior, somatosensory functions, and motor functions. With disease diagnosis taken into account, only the EMCI group indicated a decrease in global BOLD signal complexity with increased brain amyloid load.

Analysis of rs-BOLD signal complexity has the potential to provide a more accurate representation of disease state than current amyloid plaque or structural measures, as well as identify the regions altered by disease pathology. Based on the reduced signal complexity reported in regions previously linked to disease pathology (precuneus/posterior cingulate, lateral temporal lobe, and frontal regions), further study of this novel metric is advised. With validation, the BOLD complexity analysis metric can be attuned to use as a cognitive biomarker in the clinical setting, potentially improving disease diagnosis, treatment monitoring, and evaluation of future treatment options.

TABLE OF CONTENTS

LIST OF TABLES

LIST OF FIGURES

Introduction

Resting-State Functional MRI (rs-fMRI) & BOLD Signals

The resting brain contains a wealth of information on brain activity, as measurable through analysis of the synchronized oxygen-metabolism changes between functionally connected regions (Fox & Raichle 2007; Logothetis 2008; Biswal 1995). Resting-state functional magnetic resonance imaging (rs-fMRI) has been used to analyze functional network connectivity without some of the difficulties faced by task-based fMRI techniques, including *a priori* assumptions of the paradigm-disease relationship, low inter-subject reliability and intra-subject variability, external factors affecting attention to the task at hand, and lengthy scan times due to task repetitions, which are potentially altered by cognitive deficits (Fleisher 2009; Ances 2008; Logothetis 2004). The brain consumes 20% of the body's energy, yet task-based activation only accounts for approximately 5% of the energy use, leading to the belief that brain activity is best represented at resting state (Clark 1999; Fox & Raichle 2007).

The basis of resting-state fMRI measurements is the quantification of the blood-oxygen level dependent (BOLD) signal. Neuronal activation results in increased blood flow to participating regions, causing a change in concentration of oxygenated (diamagnetic, negative magnetic susceptibility) and deoxygenated hemoglobin (paramagnetic, positive magnetic susceptibility) (Raichle & Mintun 2006). Due to the opposing magnetic susceptibilities, distortion of the magnetic field and subsequent fMRI image contrast occurs (Fox & Raichle 2007; Ogawa 1990).

Since resting-state BOLD signals are believed to indirectly represent neural activity, they carry potential for use as a measure of disease-associated loss of cognitive function. The components of resting-state BOLD signals include spontaneous metabolic and neuronal fluctuations, physiological noise (cardiac and respiratory pulses), and thermal noise from the scanner (Liu C 2012; Raichle & Mintun 2006). Of these, the contrast between metabolic and neuronal spontaneous low frequency fluctuations (0.01-0.08 Hz) reflects the functional connectivity between structurally unconnected brain regions (Fox & Raichle 2007; Wang 2007).

Conventional Analysis of rs-fMRI BOLD Signals

Conventionally, resting-state fMRI data has been analyzed using correlations to infer functional connectivity within brain networks. Although this approach has been highly informative, the use of correlations rests on the fundamental assumption that BOLD fluctuations are caused by deterministic (i.e. predictable) processes, aside from small corruptions due to random noise (Fox & Raichle 2007; Raichle & Mintun 2006; Biswal 1995). This, however, seems highly restrictive given the current knowledge of how the brain functions. A more general view is that the BOLD fluctuations are caused by stochastic processes, implying that the patterns of BOLD fluctuations are irregular and to some degree unpredictable (Nierhaus 2012; Hu & Shi 2006). The overall objective of this study is to quantify the degree of irregularity in BOLD fluctuation patterns with the expectation that this approach provides new insight into normal and pathological brain activity, given that

stochastic processes are the underpinning of brain function (Nierhaus 2012; Stevens 2009; Hu & Shi 2006; Liu C 2012).

To deal with stochastic processes whose attributes are "hidden," in the sense that there is no *a priori* model for the temporal patterns, the framework of computational mechanics, a branch of information theory, was introduced (Crutchfield and Feldman, 2001; Crutchfield and Young, 1989). Here, we apply ideas from computational mechanics and corresponding measures of complex non-linear dynamics to characterize resting-state stochastic BOLD patterns. Specifically, this study aims to quantify the complexity of stochastic BOLD patterns based on how quickly pattern configurations can be identified.

Complexity Analysis of BOLD Signal Fluctuations

The proposed BOLD signal fluctuation complexity analysis metric will serve to measure the changes in cognitive activity in the selected brain regions and irregularities in functional connectivity between those regions, in an effort to identify functional changes in disease state. In these terms, complexity represents the integrity and efficiency of information processing in a system (Nakagawa 2013), and is quantified by the amount of time that it takes to identify (i.e. reduce uncertainty) the stochastic BOLD signal pattern. According to these terms, random as well as regular patterns exhibit a low degree of complexity in contrast to any less random or less regular pattern. Healthy brains should display complex time series distributed throughout multiple brain regions, with a contrasting increased

3

localization and reduced complexity in a diseased brain (Nakagawa 2013; Liu Y 2012).

The signal analysis process uses information theory, based on the previously mentioned concept of computational mechanics, to measure the evolution of stochastic systems over time (i.e. the gain in information over time) (Schreiber 2000). Since BOLD rs-fMRI signals are made up of irregular inhomogeneous and non-stationary fluctuations (i.e. not task specific), a measure of entropy can be used to represent the degree of randomness in the system (Hu & Shi 2006). Specifically, the growth rate of the system's evolution can be quantified by block entropy, which quantifies the change of uncertainty of predicting the signal pattern over time (Hu & Shi 2006). A completely random (unpredictable) or periodic (predictable) system would have a fast rate of information generation (high entropy, patterns are easy to recognize), as opposed to a more complex system (more uncertainty, slower rate, low entropy, patterns are difficult to recognize) (Liu Y 2013; Hu & Shi 2006). In the case of more complex patterns, the average number of observations needed to reduce uncertainty is increased. The resulting measure of the combined block entropy and average number of observations (i.e. average block entropy growth rate) is known as a transient information value, or TI. Periodic or random systems have a TI value close to zero, whereas complex stochastic BOLD fluctuation patterns will have increased TI values (Liu Y 2013). Accordingly, brain regions that process high amounts of information (governed by processes that are highly complex) should exhibit high TI values in comparison to regions that process low amounts of information.

Alzheimer's Disease

Alzheimer's disease is the predominant form of age-related dementia today, causing progressive degeneration of cognitive function. The primary pathology observed during the course of the disease consists of accumulation of beta amyloid plaques, tau-mediated neuronal injury (neurofibrillary tangles), and cortical and hippocampal atrophy (Jack 2010). The observed structural changes are thought to be accompanied by functional disconnection between primary networks, ultimately resulting in loss of cognitive abilities and disruption of daily functions. Regions of the Default Mode Network (DMN) and Medial Temporal Lobe (MTL) system have been shown to suffer from metabolic and functional disconnections, specifically in the hippocampus, precuneus, posterior cingulate cortex, lateral temporal lobe, and frontal lobe (Sperling 2009, Camus 2012; Greicius 2004; Das 2013). Structural changes are noted primarily in the hippocampal region, entorhinal cortex, medial temporal lobe, lateral temporal lobe, and frontal lobe areas (Kim 2013; Dickerson 2008).

Current efforts split the research focus between identifying early disease signs in hopes of earlier diagnosis and creating viable treatment options for use once the disease mechanisms are better understood. Irregularities in functional and structural connectivity between brain regions are believed to be the cause of some of the cognitive deficits observed in Alzheimer's patients, affecting working memory, episodic memory, and attention function (Delbeuck 2003; Gomez-Isla & Hyman 1997). A common method of visualizing and measuring the loss of connections is by structural imaging (MRI, CT, PET, etc.), but most discernible

structural changes are thought to occur after the disease has progressed and caused irreversible damage to the brain. Identifying early functional changes can lead to the detection of asymptomatic or prodromal Alzheimer's disease (AD), which is considered as a form of Mild Cognitive Impairment (MCI) (Camus 2012).

Currently, AD can only be confirmed through histopathology by performing a biopsy or autopsy. The classification of disease state as reported by ADNI in this study was determined through clinical criteria (McKhann 1984), based on the Clinician's interpretation of various factors including family-, self-, or clinician-reported memory concern, level of day-to-day functionality, stability of medication use, presence of other diseases, and results on cognitive assessment tests: Memory Function Weschler Memory Scale (WMS), Mini-Mental State Exam (MMSE), and Clinical Dementia Rating (CDR).

By the current disease diagnosis criteria, Controls are defined as healthy subjects who are non-depressed, non-MCI, and non-demented, with stable use of allowable medications and without a reported memory concern. Early MCI (EMCI) subjects demonstrate a slight decrease in any one cognitive test score (1 to 1.5 standard deviations below control mean on any cognitive domain), have a reported memory concern, but have a non-AD diagnosis for cognition and functionality. MCI subjects display AD cognitive deficiency symptoms to a lower degree and are at a greater risk of developing AD, as well as score 1 to 1.5 standard deviations below control mean performance on the memory domain, score lower than EMCI subjects, and have a reported memory concern, but still cannot be diagnosed with AD due to maintained levels of cognition and functionality. In AD patients, cognitive

impairment is sufficiently great, such that there is interference with daily function and low memory function test scores (McKhann 1984).

Current Study

This study implements the BOLD signal fluctuation complexity analysis technique developed by Dr. Yinan Liu from the Center for Imaging of Neurodegenerative Diseases (CIND) at the VA Medical Center and University of California, San Francisco (Liu Y 2013). The focus of this research is to use information theory to show that the BOLD signal fluctuation patterns are predictable, and determine to what extent these measures represent Alzheimer's disease state.

The function-based complexity analysis method will be compared to the pre-existing structural analysis method of brain amyloid plaque count from Positron Emission Tomography (PET) ^{18}F-AV-45 (Florbetapir) uptake, in order to test the novel biomarker's effectiveness, limitations, and the possible association with harmful amounts of brain amyloid plaque. The Gold Standard for comparison of both markers is the clinical diagnosis (Healthy Controls, EMCI, MCI, and AD) reported by the Alzheimer's Disease Neuroimaging Initiative (ADNI) database, from where all of the study data was retrieved (http://adni.loni.ucla.edu).

In this retrospective, multicenter, cross-sectional study, I expect to observe both a global and a selective regional (i.e. regions affected by disease progression) reduction in BOLD signal fluctuation pattern complexity in the presence of brain

amyloid, without regard to clinical diagnosis. I also expect to detect a reduction in BOLD signal complexity with disease progression and increased amyloid plaque.

Materials and Methods

Participants

Subjects for this study were selected from the ADNI database conditional of the availability of at least one rs-fMRI scan and PET ^{18}F-AV-45 (Florbetapir) brain amyloid data. All ADNI data passes strict quality control (QC) criteria for admission into the database. For further QC, the chosen subjects were assessed for adequate population spread and group matching characteristics (based on age, group size, gender distribution, cognitive testing (ADAS-Cog score), PET and fMRI scan time-lag, and SUVr & CSF biomarker trends), as well as multiple scan QC steps during pre-processing.

At the time of the study, complete data was available from the sixty-five subjects, comprised of 30 males and 35 females between 58 and 90 years old (mean age ± SD: 74 ± 7.4 years; Table 1). Data consisted of one set of PET-amyloid data (Screening) and one to four rs-fMRI scans (Screening, 3 months, 6 months, 1 year). Subjects were distributed across four groups by clinical diagnosis: 15 healthy controls (Control), 28 Early Mild Cognitive Impairment (EMCI), 17 Mild Cognitive Impairment (MCI), and 5 Alzheimer's disease (AD). The uneven distribution was based on availability of data, but can also be attributed to the prevalence of EMCI

and MCI diagnoses as opposed to progressed AD, which is more difficult to confidently diagnose.

The primary scope of this project is to provide a predictive metric for asymptomatic developing Alzheimer's disease, so analyzing changes in early disease state (EMCI & MCI) will be instrumental in determining functional changes before irreversible disease progression. Diagnostic groups displayed an overlap in SUVr ranges without clear cutoffs, since brain amyloid load varies between individuals, but the expected increase in brain amyloid with disease progression is present. The ranges are higher than SUVr values reported in the literature, but the relationship with disease remains consistent (Camus 2012; Fleisher 2009).

Table 1 *Demographic Characteristics of Subjects*

	Control	EMCI	MCI	AD	Total or Avg
n	15	28	17	5	65
Age (mean ± SD)	76 ± 6.2	73 ± 7.5	71 ± 6.3	79 ± 12	74 ± 7.4
% Male	53	67	59	40	46
ADAS-Cog Score* (mean ± SD)	8 ± 3.8	13 ± 5.9	19 ± 7.7	33 ± 8.5	18 ± 6.5
Total SUVr** (mean ± SD)	1.18 ± 0.25	1.21 ± 0.23	1.20 ± 0.22	1.47 ± 0.14	1.27 ± 0.21

*Alzheimer's Disease Assessment Scale (ADAS) 13 item cognitive test; Scores out of 40 possible points; Higher scores represent more mistakes.
**Standardized Uptake Value of Florbetapir in whole brain cerebellum; Representative of brain amyloid load.

Image Acquisition

All scans used in this study were acquired by ADNI-participating institutions, followed ADNI-regulated protocols, and passed the ADNI QC process. Scan parameters and protocols were obtained from the ADNI website (http://www.adni-info.org/Scientists/ADNIStudyProcedures).

PET

The ^{18}F-AV-45 uptake PET imaging protocol called for a 10 mCi (± 10%, without saline dilution) injection of Florbetapir via a 5-10 second intravenous bolus injection. The PET emission scan began 50 minutes post-injection and lasted for 20 minutes of continuous scanning (four 5-minute frames). An attenuation correction scan was performed at 40 minutes post-injection for CT-PET scanners as a CT scan, and as a transmission scan post-emission scan for PET-only scanners. Images were reconstructed directly after acquisition to allow for an immediate rescan in the case of motion or artifacts. Scans underwent a single 3D iterative reconstruction (128 x 128 grid, 256 mm FOV, 2 mm voxel size, 3.27 mm slice thickness) using filtered back projection and no smoothing filter.

rs-fMRI

For resting-state functional BOLD signal analysis, three MR scans were acquired on 3T Philips MR scanners (total scan time 7 minutes). First, a structural T1-weighted scan (TR 2300 ms, TE 3.37 ms, TI 950 ms; flip angle 7°, 1 x 1 x 1 mm³ resolution) was acquired for anatomical labeling and segmentation, using a spoiled fast gradient echo sequence during inversion recovery (MP-RAGE or IR-SPGR). Next, a 3D T2-weighted scan (TR 3000 ms, TE 356 ms, echo train 109, 1 x 1 x 1 mm³

resolution) was acquired for co-registration of the rs-fMRI and structural T1-w scans, using variable flip angle turbo spin-echo sequencing. Finally, the rs-fMRI scan (TR 3000 ms, TE 30 ms, flip angle 80°, NEX 1, 140 time points, single echo, 48 slices, 3.3 x 3.3 x 3.3 mm resolution) was acquired using a gradient-echo echo-planar imaging (GE-EPI) sequence.

Image Processing

The total cerebellum normalized Standardized Uptake Value ratio (SUVr) of ^{18}F-AV-45 from PET data was obtained directly from the ADNI database and used as a direct measure of brain amyloid load. The rs-fMRI raw images were obtained raw, and were processed and analyzed for the BOLD signal complexity analysis measure. As a global comparison, the primary analysis requires only one rs-fMRI scan, for which the scan acquired closest to the PET acquisition date (typically 1 month after the Screening fMRI acquisition) was selected. Future studies may implement a longitudinal comparison of complexity changes based on all available fMRI scans, but for this study, only the initial diagnosis and PET data was available for comparison.

PET

The ^{18}F-AV-45 PET scans were processed by Dr. William Jagust's laboratory of the Helen Wills Neuroscience Institute, of UC Berkeley and Lawrence Berkeley National Laboratory. The scans were processed with the FreeSurfer image analysis suite (http://surfer.nmr.mgh.harvard.edu/), using cutoff values derived from the data to determine regional and total Florbetapir SUV ratios. The regions of interest

reported for amyloid count included cortical grey matter uptake averages (frontal, cingulate, parietal, and temporal), as well as reference regions (brainstem, cerebellar grey matter, whole cerebellum), and the whole cerebellum normalized uptake. For the purposes of this study, the whole cerebellum normalized SUVr will represent the whole brain amyloid load.

rs-fMRI

The rs-fMRI series were downloaded in 4D NIfTI format from the ADNI database and then split into 3D slices for ease of processing. The pre-processing steps of the rs-fMRI scans implemented in this study are consistent with previously reported analysis methods (Chao-Gan & Yu-Feng 2010; Vergun 2013). Rs-fMRI image processing was performed using tools in the SPM8 software package (Wellcome Institute of Cognitive Neuroscience, London UK), MATLAB (The MathWorks, Inc., Massachusetts US), and R Project statistical analysis program (http://www.r-project.org/).

First, each subject's selected fMRI scan underwent removal of unnecessary leading data (20 out of 140 time points), followed by slice-timing correction, to offset the EPI sequence 3 second difference between acquisition of the first and last slices and to correct for gaps. Next, realignment of the time series was performed based on the estimation of misalignment and re-slicing to correct for subject motion. Spatial smoothing with an isotropic 8 mm Gaussian Kernel was applied to the output image to increase the signal-to-noise ratio (SNR). Next, the T1-weighted scan from FreeSurfer was co-registered to the fMRI scan with the parcelated T1 image as an intermediate, via nearest neighbor interpolation. The coregistered image then

undergoes a visual QC to verify alignment of coordinates between all image types. Following this, a bandpass frequency filter was applied to remove low-frequency noise (0.01 to 0.08 Hz), followed by linear detrending to remove signal changes from remaining physiologic noise.

After preparation of the rs-fMRI images, the complexity analysis method was applied to compare the BOLD signal fluctuation patterns, following the steps developed by Dr. Yinan Liu (2013), using the Flexmix and AnalyzeFMRI packages from the R Project statistical analysis program. Per subject, the complexity analysis code splits the fluctuations within each voxel into 20 bins (within the range of 20-60, determined from the estimated relationship between regional TI values). Then, block entropy (H(L)), excess entropy (EE), and transient information (TI(L)) maps are created for the entire brain. The TI values from the TI(L) map, after segmentation into 82 FreeSurfer cortical and subcortical grey matter regions (Figure 1), serves as a measure of regional signal complexity for each subject.

Statistical Analysis

The regional BOLD complexity scores (TI) and whole brain normalized (SUVr) values were evaluated to test the two hypotheses of this study. First, the global BOLD signal complexity was determined by averaging data from the 82 cortical and subcortical grey matter regions, per subject. To assess the relationship between overall signal complexity and brain amyloid load, the global complexity values were then compared to the respective whole brain normalized SUVr, without regard of clinical group. To test the effect of brain amyloid on BOLD signal

complexity across clinical diagnosis group, the global SUVr and complexity values were separated by group and compared.
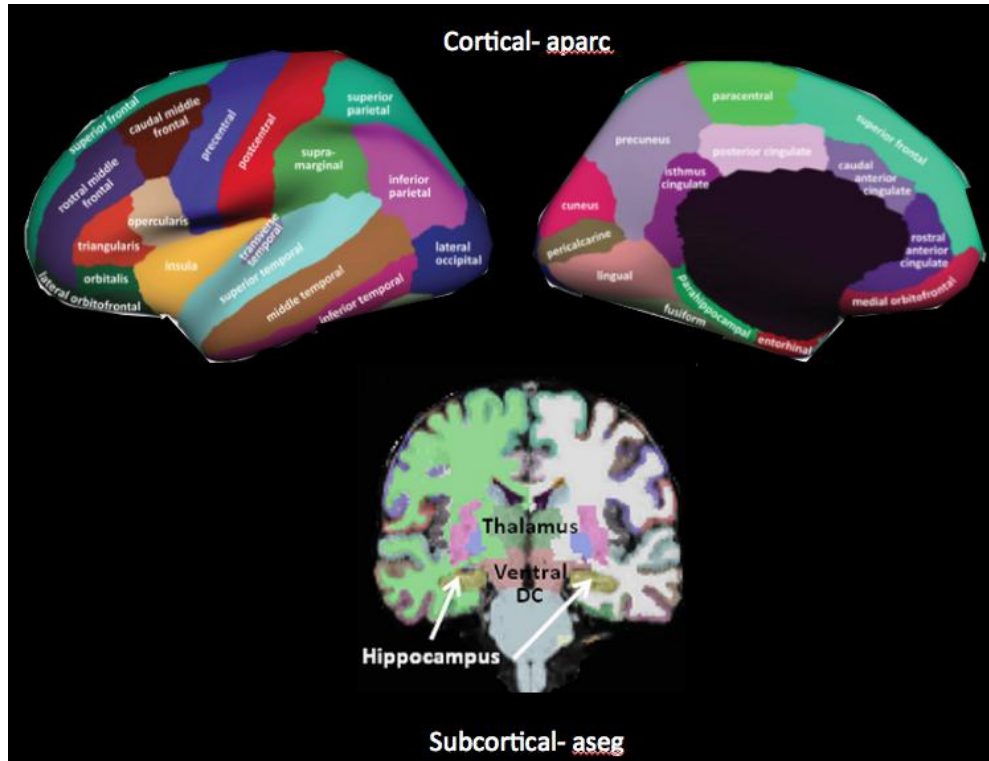
Next, to determine if certain brain regions were more altered than others, the regional relationship between complexity and total brain amyloid load was analyzed. Complexity scores (TI) from all subjects, regardless of clinical group, were evaluated with a linear mixed effects model that separated between and within subject variability across regions. In addition, variations in TI were covariate for age and presence of APOE4 alleles and referenced to the complexity of the bilateral

thalamus region. The effect of brain amyloid on signal complexity was shown to be significant in some regions, with negative correlations between TI scores and brain amyloid load (i.e. decreasing TI values as amyloid load increases). The strength of the association between the two factors was determined at the 90, 95, 98, and 99% confidence levels.

Results and Discussion

Global BOLD Signal Complexity and Brain Amyloid

For all subjects, without respect to clinical diagnosis, the global comparison of BOLD signal complexity (TI) and brain amyloid (SUVr) showed a non-significant trend toward increased signal complexity with higher amounts of brain amyloid load (Figure 2). The distribution of complexity scores is seen to focus around the low to medium range (10-30), and the SUVr values are distributed within the 0.95-1.75 range. Also, dense clusters are noted in the low to medium complexity, low to medium amyloid area.

Regional BOLD Signal Complexity and Brain Amyloid

Twenty-seven out of the eighty-two selected cortical and subcortical grey matter regions were found to have a significant (>90% CI) effect of brain amyloid load on BOLD signal complexity (Table 2). Of the affected regions, the putamen, pallidum, caudate nucleus, anterior cingulate gyrus, and pars opercularis regions

15

showed the highest negative association (>99% CI) of signal complexity with brain amyloid.
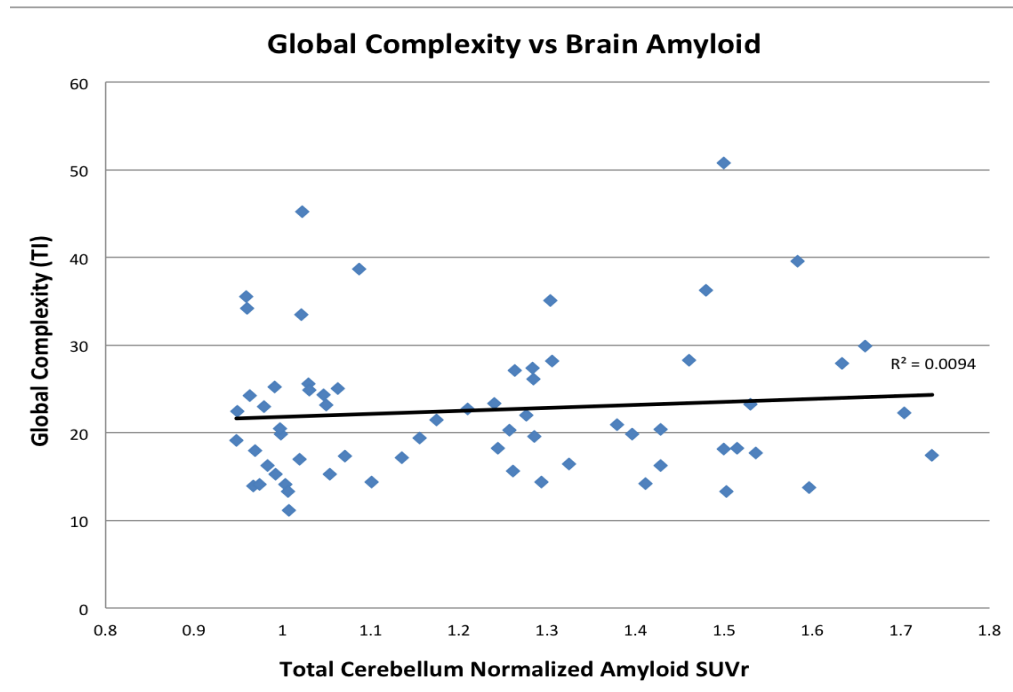

Figure 2. Comparison of the global BOLD signal complexity values (TI) to the total cerebellum normalized florbetapir uptake (SUVr). BOLD signal complexity is observed to increase slightly (<1%) with increasing brain amyloid.

Diagnostic Group Comparison

With clinical diagnosis taken into account, the trends of the disease population were compared to that of the control population (Figure 3). The Control group shows a spread of complexity values widely distributed throughout the full SUVr range, with a cluster in the low to medium complexity, low amyloid range. The highest complexity values are also from the Control group.

Table 2 *BOLD Signal Complexity Reduction by Whole Brain Normalized Amyloid (SUVr)*

Region	t value	Functional Effects	Structural Connections	Source
Cortical				
R Entorhinal Cortex	2.179[b]	Episodic memory, memory formation & consolidation	MTL; hippocampus	Sperling 2009
L Precuneus	1.922[a]	Episodic memory, visuospatial processing, consciousness	DMN; hippocampus	Greicius 2004
R Frontal Pole	1.805[a]	Attention, task monitoring	Prefrontal cortex	Koechlin 2011
L Superior Frontal Cortex	1.799[a]	Visuo-spatial working memory	Frontal & Parietal lobes	Klingberg 2006
R Caudal Middle Frontal	2.000[b]	Attention, working memory	Frontal & Parietal lobes	Neufang 2011
R Rostral Middle Frontal	2.347[c]			
R Lateral Orbitofrontal	2.096[b]	Sensory (taste, olfaction), decision making, behavior, emotion, autonomic function	Amygdala & hippocampus	Van Hoesen 2000
R Precentral Gyrus	2.555[c]	Motor control	Primary motor cortex; posterior frontal lobe	Bonni 2013
L Postcentral Gyrus	2.404[c]	Somatosensory	Primary somatosensory cortex	Bonni 2013
L Paracentral Lobule	2.081[b]	Motor & somatosensory	Frontal & Parietal lobes	Bonni 2013
R Temporal Pole	1.677[a]	Attention, emotion, behavior, episodic & declarative memory	Limbic system	Blaizot 2010
R Inferior Temporal Gyrus	1.741[a]	Language	Temporal lobe	Scheff 2011
L Superior Parietal	2.309[b]	Visuo-spatial processing, long-term & working memory, sensorimotor	Posterior parietal cortex	Koenigs 2009, Wolpert 1998
R Superior Parietal	2.499[c]			
L Caudal Anterior Cingulate	2.992[d]	Emotional regulation, motivation, autonomic functions, behavior	Amygdala & hippocampus	Etkin 2011
R Rostral Anterior Cingulate	2.866[d]			
L Supramarginal Gyrus	3.643[e]	Language perception & processing	Parietal Lobe	Penniello 1995
R Supramarginal Gyrus	2.370[c]			
R Pars Triangularis	2.351[c]	Speech & language comprehension	Inferior Frontal Gyrus; Broca's area	Greenlee 2007
L Pars Opercularis	2.212[b]			
R Pars Opercularis	3.105[d]			
R Pars Orbitalis	1.819[a]			
Subcortical				
L Pallidum	2.748[d]	Motor control		Jong 2008
R Pallidum	2.765[d]			
L Putamen	3.885[e]	Motor control, reinforcement learning & implicit learning	Basal Ganglia; limbic loop (Hippocampus & Thalamus)	Jong 2008
R Putamen	1.893[a]			
L Caudate Nucleus	3.188[d]	Learning & memory (feedback processing), emotion, language comprehension		Grahn 2008

[a] p < 0.1, [b] p < 0.05, [c] p < 0.02, [d] p < 0.01, [e] p < 0.001

Taken together, the disease groups display an even spread throughout the amyloid range, with higher density of subjects in the low to medium complexity range. In the EMCI group, complexity is seen to decrease with increased amyloid load (Figure 4), as predicted. In contrast, for the MCI group, there is an overall trend of rising complexity with an increase in amyloid load (Figure 5). Additionally, MCI subjects become less prevalent and more distributed in the high amyloid load region. With only 5 subjects, it is difficult to determine statistically whether the AD group shows a significant effect, but the subjects are noted in the high amyloid range, with medium to high complexity values.

As expected, the group averages of total brain amyloid load increased with disease progression (Table 3). Surprisingly, the average global complexity values for the disease groups also increased with disease progression, whereas the Control group showed a large variation.

Table 3 *Diagnostic Group Comparison*

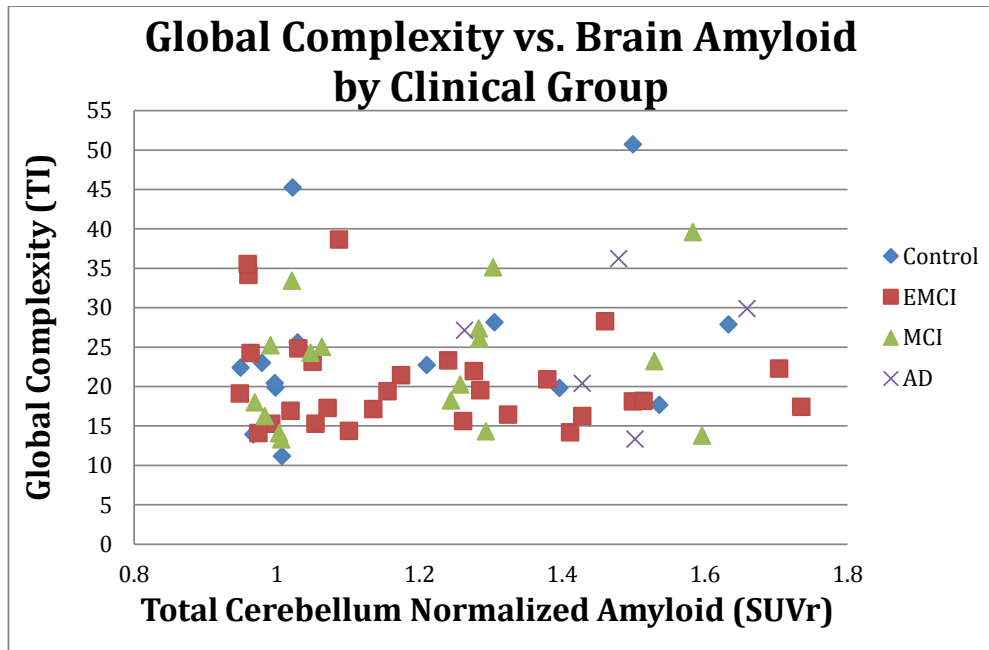| Group	Avg TI	Avg SUVr
Control	24.9 ± 10.9	1.18 ± 0.25
EMCI	20.8 ± 6.4	1.21 ± 0.23
MCI	22.8 ± 7.9	1.20 ± 0.22
AD	25.4 ± 8.8	1.47 ± 0.14

Figure 3. Comparison of global BOLD signal complexity values (TI) to total cerebellum normalized florbetapir uptake (SUVr) by clinical diagnosis.
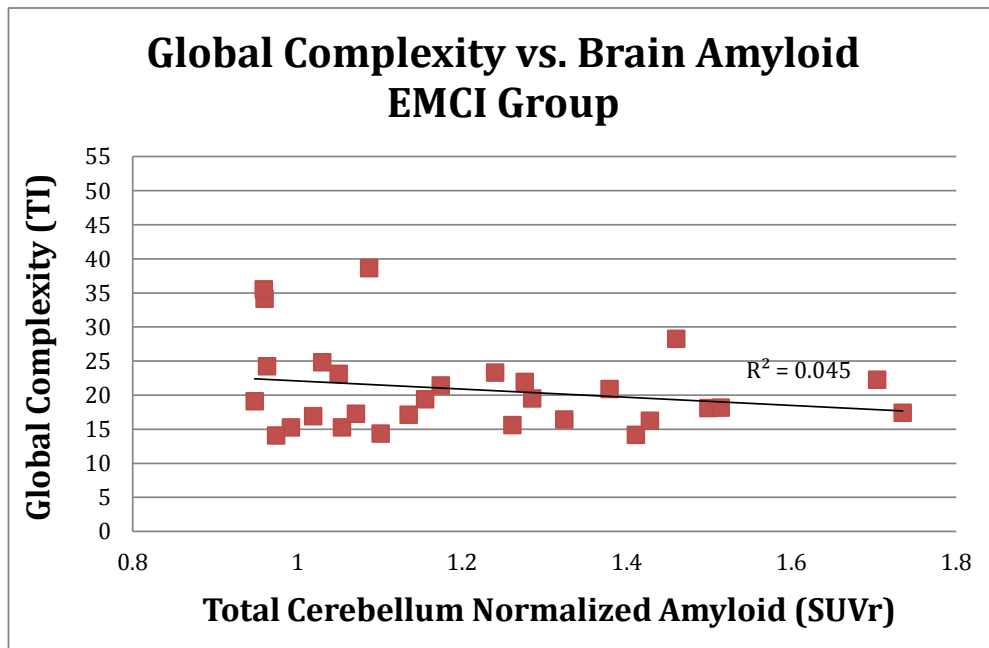

Figure 4. Comparison of global BOLD signal complexity values (TI) to total cerebellum normalized florbetapir uptake (SUVr) for Early Mild Cognitive Impairment group; showing a decrease in signal complexity with increasing brain amyloid.
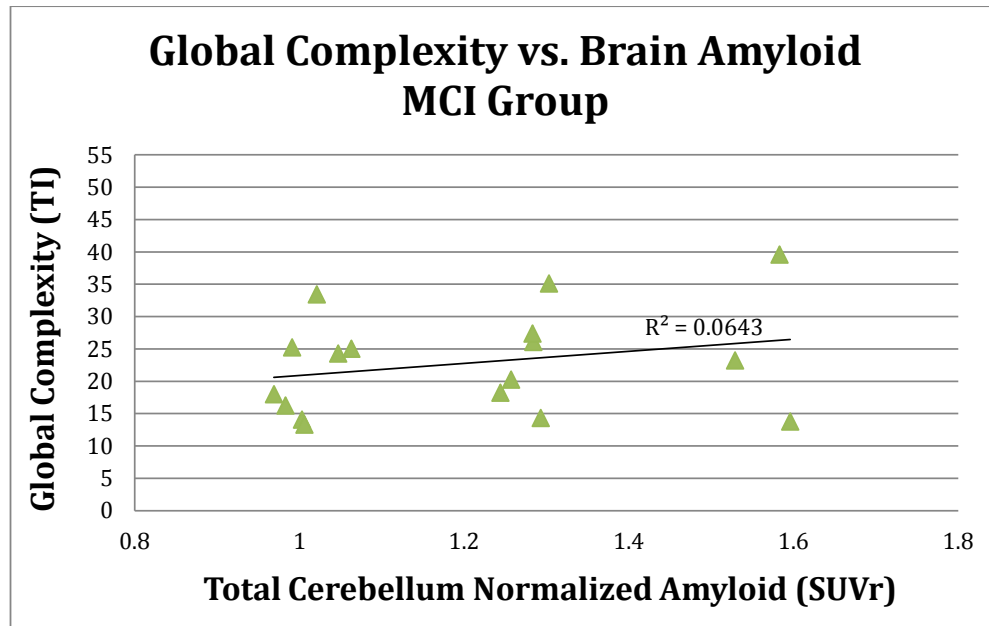
Figure 5. Comparison of global BOLD signal complexity values (TI) to total cerebellum normalized florbetapir uptake (SUVr) for Mild Cognitive Impairment (MCI) group; showing an increase in signal complexity distribution with increased brain amyloid.

Discussion of Main Findings

The main findings in this study were consistent with the hypothesized regional reduction in functional complexity with increasing amyloid burden, regardless of disease. However, global changes in functional complexity were not fully consistent with the expected relationship with increased amyloid burden, despite diagnostic group differences.

The regional relationship found in this study, as summarized in Table 2, best represents the effect of neurodegenerative amyloid plaque pathology on the cognitive processes. Various regions with structural or functional connections to regions with known association with Alzheimer's disease symptoms (i.e. hippocampus, limbic system, basal ganglia, Medial Temporal Lobe, and Default

20

Mode Network) were identified. Cognitive and functional changes caused by Mild Cognitive Impairment and Alzheimer's disease damage include memory loss, the inability to process and form new memories, behavior changes, language issues, as well as loss of motor control, sensory perception, and control of bodily functions.

In this study, reduced complexity was observed in many regions associated with these changes. Specifically, cognitive changes (i.e. memory dysfunction and language processing) can be linked to the effect observed in the entorhinal cortex, precuneus, caudate nucleus, superior & inferior frontal cortex, mid-frontal cortex, and temporal & parietal regions (Sperling 2009; Greicius 2004; Grahn 2008; Klingberg 2006; Greenlee 2007; Neufang 2011; Blaizot 2010; Koenigs 2009; Wolpert 1998; Penniello 1995; Scheff 2011). Attention and behavioral dysfunction can be attributed to the changes reported in the frontal and temporal regions, caudate nucleus, and anterior cingulate (Koechlin 2011; Neufang 2011; Van Hoesen 2000; Blaizot 2010; Etkin 2011; Grahn 2008). In addition, somatosensory and sensorimotor alterations are connected to the changes in the orbitofrontal area, precentral & postcentral gyri, paracentral area, and basal ganglia region (Jong 2008; Van Hoesen 2000; Bonni 2013).

The results of the global comparison of brain amyloid and BOLD signal complexity show a spread of mostly low to medium complexity values throughout the brain amyloid range. This spread most likely occurs due to the averaging of all selected brain regions, which includes both high activity regions and low activity regions. Another possible explanation is that the divergence in the relationship between BOLD signal complexity and amyloid load reflects compensatory

activations in some brain regions in response to compromised functions in other regions. To further explore this possibility, an evaluation of the regional complexity variations is warranted. The cluster of global complexity values in the low to medium range further supports the possibility of averaged effects. Also, a partial volume effect from white matter and CSF inclusion due to the use of large anatomical ROIs has potentially contributed to this problem. Studies involving the correction of partial volume effect will be necessary to determine the extent to which structural variations mimic changes in functional complexity.

When the global effect is separated by clinical diagnosis, some trends begin to become apparent. In terms of the brain amyloid and disease state relationship, the majority of subjects are distributed throughout the range, with a clustering of both control and disease-state subjects in the low to medium amyloid area. This supports the need for a more specific measure of disease detection and staging, as the variation between subjects does not appropriately represent dysfunction. The majority of AD subjects are found in the high amyloid range, and a cluster of Control subjects is present in the low amyloid range, which follows more closely with the expected trends. In terms of BOLD signal complexity, the Control and EMCI subjects have the highest values, which supports the theory that BOLD signal complexity declines with increasing stages of cognitive impairment. The EMCI group, which is best represented in this study due to a higher sample size (43% of the selected sample), displays the expected decrease in overall signal complexity with the increase in brain amyloid.

Limitations and Future Studies

The sensitivity of this study was constrained by the small sample size of 65 subjects, which limits the ability to generalize regional changes to larger populations. However, the regional effects were consistent with Alzheimer's disease pathology. Further studies should be implemented to test this metric, with larger sample sizes for all groups, specifically with better representation of subjects diagnosed with Alzheimer's disease.

The previously mentioned limitation of partial volume effects (PVE) may have confounded variations in complexity, especially in subjects who also present brain atrophy. PVE corrections need to be developed for complexity measures in rs-fMRI to exclude the possible resulting imitation of complexity changes.

The use of averaged complexity values over large anatomical regions does not account for the heterogeneity of a functional measure of signal complexity within each region. To take this into account, voxel-wise analysis or histogram analysis can be used to define smaller and more homogenous regions. However, this correction method may come at a loss of statistical power due to the requirement to control for the rate of false positives from the increased number of tests.

Due to the previously mentioned overlap of the large anatomical ROIs into white matter and CSF regions, complexity values can be underestimated or averaged out. To correct for this problem, partial volume correction can be performed, as well as filtering out voxels based on weighting of grey matter. Also, a comparison of fewer regions, selected based on *a priori* knowledge of disease pathology, can increase the specificity of the results to disease-related changes. Also, the regions

would correspond better to the functional metric used in this study if they were defined by functional ROIs, such as Broadmann areas.

Looking at a global measure in a cross-sectional study suffers from inter-subject variability, resulting in averaged effects and variability that is not directly related to disease state. Global functional complexity changes would be better represented in a longitudinal study, where intra-subject variability can be tested to see changes with disease progression.

To improve the transient information complexity measure, dynamic binning should be considered. The current method tested the effectiveness of the metric using a set 20-bin split of the voxels for each subject, whereas future methods could change the bin size for each subject. This would avoid having all of the values fall into the bottom few bins in low signal regions.

For further assessment, the distinction between complexity changes due to increased randomness or synchrony should be tested, based on the distribution of eigenvalues throughout the time series. Presumably, observing a broader distribution will correlate to randomness of fluctuations, thereby specifying the TI metric further.

Conclusion

Early detection of Alzheimer's disease is paramount for effective disease modifying intervention (once such treatment becomes available) before disease progression leads to irreversible brain damage.

The goal of this study follows the primary goal of the Alzheimer's Disease Neuroimaging Initiative: to identify a robust biomarker of the disease for accurate detection. The proposed measure of functional complexity serves this purpose by quantifying the reduction in stochastic BOLD signal patterns at rest, which is representative of cognitive changes. With validation, the BOLD complexity analysis metric can be implemented as a cognitive biomarker in the clinical setting, with potential uses varying from recognition of functional changes in diagnosis, monitoring of treatment and disease progression, as well as assessment of potential treatment options.

The signal complexity analysis method then has the potential to be expanded to analyze changes that occur in other neurodegenerative diseases, (i.e. Parkinson's disease), where *a priori* knowledge of functionally-altered areas can direct the identification of early changes. For diseases with unknown sources or patients with unknown diagnoses, this method may assist by searching for regional changes in functional activity then making connections to the disease state.

Analysis of the resting-state BOLD signal complexity has the potential to provide a more accurate representation of disease state than current amyloid plaque or structural measures, as well as identifying the specific regions universally affected in the progression of AD. Current efforts focus on detecting early disease changes in the precuneus/posterior cingulate, lateral temporal lobe, and later changes in the frontal regions. Based on the effects seen in these regions using the BOLD signal complexity analysis measure, efforts to improve and further study this novel metric would be suitable.

References:

Ances BM, et al., 2008. Regional differences in the coupling of cerebral blood flow and oxygen metabolism changes in response to activation: implications for BOLD-fMRI. Neuroimage 4, 1510-1521.

Biswal B, et al., 1995. Functional connectivity in the motor cortex of resting human brain using echo-planar MRI. Magnetic Resonance in Medicine 4, 537-541.

Blaizot X, et al., 2010. The human parahippocampal region: I. Temporal pole cytoarchitectonic and MRI correlation. Cerebral Cortex 20, 2198-2212.

Bonni S, et al., 2013. Altered parietal-motor connections in Alzheimer's disease patients. J Alzheimer's Dis 33, 525-533.

Camus V, et al., 2012. Using PET with 18F-AV-45 (florbetapir) to quantify brain amyloid load in a clinical environment. Eur J of Nuc Med and Mol Imaging 39, 621-631.

Chao-Gan Y & Yu-Feng Z, 2010. DPARSF: a MATLAB toolbox for "pipeline" data analysis of resting-state fMRI. Frontiers in Systems Neuroscience 4, 1-7.

Clark DD & Sokoloff L, 1999. Basic Neurochemistry: Molecular, Cellular, and Medical Aspects. Philadelphia, Lippincott.

Crutchfield JP & Feldman DP, 2001. Synchronizing to the environment: information-theoretic constraints on agent learning. Advances in Complex Systems 4, 251-264.

Crutchfield JP & Young K, 1989. Inferring statistical complexity. Phys Rev Lett 63, 105-108.

Das SR, et al., 2013. Increased functional connectivity within Medial Temporal Lobe in Mild Cognitive Impairment. Hippocampus 23, 1-6.

De Jong LW, et al., 2008. Strongly reduced volumes of putamen and thalamus in Alzheimer's disease: an MRI study. Brain 131, 3277-3285.

Delbeuck X, Van der Linden M, Collete F, 2003. Alzheimer's disease as a disconnection syndrome? Neuropsychol Rev 13, 79-92.

Dickerson BC, Sperling RA, 2008. Functional abnormalities of the medial temporal lobe memory system in mild cognitive impairment and Alzheimer's disease: Insights from functional MRI studies. Neuropsychologia 46, 1624-1635.

Etkin A, Egner T, Kalisch R, 2011. Emotional processing in anterior cingulate and medial prefrontal cortex. Trends Cogn Sci 15, 85-93.

Fleisher AS, Sherzai A, Taylor C, Langbaum JBS, Chen K, Buxton RB, 2009. Resting-state BOLD networks versus task-associated functional MRI for distinguishing Alzheimer's disease risk groups. Neuroimage 47, 1678-1690.

Fox MD & Raichle ME, 2007. Spontaneous fluctuations in brain activity observed with functional magnetic resonance imaging. Nature 8, 700-710.

Gomez-Isla T, Hyman BT, 1997. Connections and cognitive impairment in Alzheimer's disease. Connections, Cognition, and Alzheimer's Disease, Hyman BT, Duyckaerts C, Christen Y, (ed), Berlin: Springer, pp 149-166.

Grahn JA, Parkinson JA, Owen AM, 2008. The cognitive functions of the caudate nucleus. Prog Neurobio 86, 141-155.

Greenlee JDW, et al., 2007. Functional connections within the human inferior frontal gyrus. J of Comparative Neurology 503, 550-559.

Greicius MD, et al., 2004. Default-mode network activity distinguishes Alzheimer's disease from healthy aging: evidence from functional MRI. Proc Natl Acad Sci 13, 4637-4642.

Hu Z, Shi P. Complexity analysis of fMRI time sequences. In proceeding of: Proceedings of the International Conference on Image Processing, ICIP 2006, October 8-11, Atlanta, Georgia, USA.

Jack CR Jr, et al., 2010. Hypothetical model of dynamic biomarkers of the Alzheimer's pathological cascade. Lancet Neurol 9, 119-128.

Kim J, Kim YH, Lee JH, 2013. Hippocampus-precuneus functional connectivity as an early sign of Alzheimer's disease: A preliminary study using structural and functional magnetic resonance imaging data. Brain Research 1495, 18-29.

Klein A & Tourville J, 2012. 101 labeled brain images and a consistent human cortical labeling protocol. Front Neurosci 6, 1-12.

Klingberg T, 2006. Development of a superior frontal-intraparietal network for visuo-spatial working memory. Neuropsychologia 44, 2171-2177.

Koechlin E, 2011. Frontal pole function: what is specifically human? Trends in Cognitive Sciences 15, 241.

Koenigs M, Barbey AK, Postle BR, Grafman J, 2009. Superior parietal cortex is critical for the manipulation of information in working memory. J Neuroscience 29, 14980-14986.

Liu C, et al., 2012. Complexity and synchronicity of resting state Blood Oxygenation Level-Dependent (BOLD) Functional MRI in normal aging and cognitive decline. J of Magn Reson Imaging , 1-10.

Liu Y, Young K, Tosun D, Zhang Y, Schuff N, 2013. Mapping Degrees of Temporal Complexity in Resting-State BOLD Fluctuations. Unpublished manuscript.

Logothetis NK & Wandell BA. 2004. Interpreting the BOLD signal. Annu. Rev. Physiol. 66:735-769.

Logothetis NK, 2008. What we can do and what we cannot do with fMRI. Nature 453, 869-878.

McKhann G, et al., 1984. Clinical diagnosis of Alzheimer's disease: Report of the NINCDS-ADRDA Work Group under the auspices of Department of Health and Human Services Task Force on Alzheimer's Disease. Neurology 34, 939-944.

Nakagawa TT, Jirsa VK, Spiegler A, McIntosh AR, Deco G, 2013. Bottom up modeling of the connectome: Linking structure and function in the resting brain and their changes in aging. Neuroimage 89: 318-329.

Neufang S, et al., 2011. Disconnection of frontal and parietal areas contributes to impaired attention in very early Alzheimer's disease. J Alzheimers Dis 25, 309-321.

Nierhaus T, Margulies D, Long X, Villringer A, 2012. fMRI for the assessment of functional connectivity. Neuroimaging - Methods, Peter Bright (Ed.), Rijeka, Croatia: InTech, pp. 29-46.

Ogawa S, et al., 1990. Brain magnetic resonance imaging with contrast dependent on blood oxygenation. Proc Natl Acad Sci 24, 9868-9872.

Penniello MJ, et al., 1995. A PET study of the functional neuroanatomy of writing impairment in Alzheimer's disease: The role of the left supramarginal and left angular gyri. Brain 118, 697-706.

Raichle ME & Mintun MA, 2006. Brain work and brain imaging. Annu Rev Neurosci 29, 449-476.

Scheff SW, Price DA, Schmitt FA, Scheff MA, Mufson EJ, 2011. Synaptic loss in the inferior temporal gyrus in mild cognitive impairment and Alzheimer's disease. J Alzheimers Dis 24, 547-557.

Schreiber T, 2000. Measuring Information Transfer. The American Physical Society 85, 461-465.

Sperling RA, et al., 2009. Functional alterations in memory networks in early Alzheimer's disease. Neuromol Med 12, 27-43.

Stevens WD, Buckner RI, Schacter L, 2009. Correlated low-frequency BOLD fluctuations in the resting human brain are modulated by recent experience in category-preferential visual regions. Cerebral Cortex 20, 1997-2006.

Strangman GE, et al., 2010. Regional brain morphometry predicts memory rehabilitation outcome after traumatic brain injury. Front Hum Neurosci 4, 1-11.

Van Hoesen GW, Parvizi J, Chu CC, 2000. Orbitofrontal cortex pathology in Alzheimer's disease. Cerebral Cortex 10, 243-251.

Vergun S, et al., 2013. Characterizing functional connectivity differences in aging adults using machine learning on resting state fMRI data. Frontiers in Computational Neuroscience 7, 1-20.

Wang KM, et al., 2007. Altered functional connectivity in early Alzheimer's disease: a resting-state fMRI study. Hum Brain Mapp 10, 967-978.

Wolpert DM, Goodbody SJ, Husain M, 1998. Maintaining internal representations: the role of the human superior parietal lobe. Nature Neuroscience 1, 529-533.
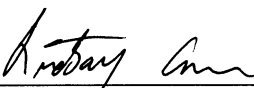
Publishing Agreement

It is the policy of the University to encourage the distribution of all theses, dissertations, and manuscripts. Copies of all UCSF theses, dissertations, and manuscripts will be routed to the library via the Graduate Division. The library will make all theses, dissertations, and manuscripts accessible to the public and will preserve these to the best of their abilities, in perpetuity.

Please sign the following statement:

I hereby grant permission to the Graduate Division of the University of California, San Francisco to release copies of my thesis, dissertation, or manuscript to the Campus Library to provide access and preservation, in whole or in part, in perpetuity.

_____   09/09/2013
Author Signature   Date